

# Histological validation of the brain cell body imaging with diffusion MRI at ultrahigh field

Marco Palombo<sup>1</sup>, Daniel Nunes<sup>2</sup>, Daniel C. Alexander<sup>1</sup>, Hui Zhang<sup>1</sup>, Noam Shemesh<sup>2</sup>.

<sup>1</sup> Centre for Medical Image Computing, Department of Computer Science, University College London, London, UK

<sup>2</sup> Champalimaud Research, Champalimaud Centre for the Unknown, Lisbon, Portugal.

## SYNOPSIS

Biophysical modelling of diffusion-weighted MRI (DW-MRI) data can help to gain more insight into brain microstructure. However, models need to be validated.

This work validates a recently-developed technique for non-invasive mapping of brain cell-body (soma) size/density with DW-MRI, by using ultrahigh-field DW-MRI experiments and histology of mouse brain. Predictions from numerical simulations are experimentally confirmed and brain's maps of MR-measured soma size/density are shown to correspond very well with histology. We provide differential contrasts between cell layers that are less expressed in tensor analyses, leading to novel complementary contrasts of the brain tissue. Limitations and future research directions are discussed.

## INTRODUCTION

Mapping brain microstructure noninvasively using diffusion-weighted MRI (DW-MRI) remains a formidable challenge due to the complexity of the underlying constituents and the relatively featureless diffusion-driven signal decay. Biophysical modelling can help to gain more insight into the microstructure<sup>1-3</sup>. However, it is very difficult to choose the correct model<sup>4</sup>, and validation is necessary.

This work validates a recently-developed technique<sup>5</sup> for non-invasive mapping of brain cell-body (namely soma) size and density with DW-MRI.

Advanced Monte-Carlo simulations, based on a recently-proposed framework<sup>6</sup>, showed that soma size/density may have a specific signature on the direction-averaged DW-MRI signal  $S_{ave}$  at high b-values<sup>5,7</sup>. Simulations also suggested that at diffusion times  $t_d < 30$  ms, the water exchange between neurites and soma may be neglected, supporting the design of a simple three-compartment model to quantify the presence of soma<sup>5</sup>:

$$S_{ave}(b)/S(b=0) = f_{sticks} S_{sticks}(b, D_a) + f_{sphere} S_{sphere}(b, D_{sphere}, R_{sphere}) + (1 - f_{sticks} - f_{sphere}) S(b, D_{iso}) \quad [1]$$

where  $f_{sticks}$  represents the MR cell-fibres signal fraction,  $D_a$  axial diffusivity;  $f_{sphere}$  MR soma signal fraction,  $R_{sphere}$  soma radius,  $D_{sphere}$  and  $D_{iso}$  intra-soma and extra-cellular diffusivity.

Here we use ultrahigh field DW-MRI and histology of mouse brain to validate those simulation results<sup>7</sup> and the proposed compartment model<sup>5</sup>.

## METHODS

**Simulations.** Detailed three-dimensional geometries were constructed to mimic realistically connected neurites, in different soma size/volume fraction ( $r_{soma}, f_{soma}$ ) conditions, as proposed in<sup>5-7</sup> (**Fig.1a**). The  $S_{ave}(b)$  signals, as measured by a Pulsed-Gradients-Spin-Echo (PGSE) sequence, were computed in CAMINO<sup>8</sup> for b-values=[0:1:40] ms/ $\mu\text{m}^2$ ,  $\delta/\Delta=3/11$  ms and direction-average across 40 gradient directions (**Fig.1b**). Only intracellular water diffusion was simulated. However, the effect of extracellular diffusion and membrane permeability were shown to be negligible at very high b-values<sup>9</sup> and diffusion times  $< 20$  ms<sup>10</sup>.

**Specimen preparation.** All animal experiments were preapproved by the institutional and national authorities and were carried out according to European Directive 2010/63. Mice (N=2), male, 8 weeks old, were perfused intracardially with 4% paraformaldehyde. The brains were isolated and kept 48h in 4% paraformaldehyde and 5 days in PBS (changed daily), before being transferred to a 10 mm NMR tube filled with Fluorinert (Sigma Aldrich) for susceptibility matching. Upon MRI, tissue was used for microscopy as described in<sup>11</sup> to provide histological benchmark.

**MRI experiments.** All experiments were performed using a 16.4 T MRI scanner (Bruker BioSpin, Karlsruhe, Germany) operating at 700 MHz for  $^1\text{H}$  nuclei equipped with a micro5 imaging probe with maximum gradient strength 3000 mT/m isotropically. The brain was kept at constant temperature of 37°C. DW-MRI were acquired using a PGSE sequence with: TE/TR=20/2500 ms;  $\delta/\Delta=3/11$  ms;  $b=0,1,2,3,5,8,10,12,16,20,25,40$  ms/ $\mu\text{m}^2$ ; 40 gradient directions, resolution 50x50x250  $\mu\text{m}^3$ , 10 slices, 4 averages.

**Data preprocessing and analysis.** Data were denoised using MP-PCA<sup>12</sup> and Gibbs ringing corrected<sup>13</sup>. No artifacts from movement or eddy-current were observed. Data at  $b=3$  ms/ $\mu\text{m}^2$  were used to compute diffusion tensor imaging (DTI) maps in mean diffusivity (MD) and fractional anisotropy (FA), using FSL<sup>14</sup>. Relation [1] was voxel-wise fitted to the measured  $S_{\text{ave}}(b)$  signal to estimate  $f_{\text{sticks}}$ ,  $D_a$ ,  $f_{\text{sphere}}$ ,  $R_{\text{sphere}}$ ,  $D_{\text{iso}}$ , fixing  $D_{\text{sphere}}=3$   $\mu\text{m}^2/\text{ms}$ .

## RESULTS

**Simulations vs. experiments.** Simulations predicted that, at  $\Delta=11$  ms,  $S(b^{-1/2})$  shows specific curvature in the range  $0.2 < b^{-1/2} < 0.5$  induced by specific  $(r_{\text{soma}}, f_{\text{soma}})$  conditions (**Fig.1b**). In agreement, the signal decay extracted from ROIs known to have different  $(r_{\text{soma}}, f_{\text{soma}})$  conditions, like Corpus-Callosum white matter (WM) and cortical gray matter (GM), reveals that these are correct (**Fig.1b**).

**MR measured features.** **Fig.2a** shows  $f_{\text{sphere}}$ ,  $R_{\text{sphere}}$  and  $f_{\text{sticks}}$  maps, for the two mouse brains. Note the exquisite differential contrasts between layers in the olfactory bulb, cortex, hippocampus and cerebellum. These contrasts are less expressed in DTI maps (**Fig.2b**).

**Comparison against histology.** A direct comparison of the MR maps with histology of the same brain is shown in **Fig.3b** and **4**. We observe very good correspondence between soma and cell-fibres spatial distributions from histology and  $f_{\text{sphere}}$ ,  $R_{\text{sphere}}$  and  $f_{\text{sticks}}$  maps. Quantitative analysis in **Fig.5** shows higher correlation of  $f_{\text{sphere}}$  with DAPI staining than MD. Comparison against literature-derived histology<sup>15</sup> is also provided in **Fig.3a**. Overall, the predicted brain's composition in terms of MR-measured soma size/density corresponds very well with ground-truth histological measurements.

## DISCUSSION and CONCLUSION

Using high resolution DW-MRI data and histology, this work confirms the predictions of numerical simulation<sup>6,7</sup> (**Fig.1**), and validate the source of new contrasts specifically related to soma size/density<sup>5</sup> (**Fig.3-5**). These are dissimilar to the simple tensor analyses (**Fig.2-5**), and therefore represent new complementary information on the brain.

Future work will investigate possible bias on parameters estimates due to cross-correlation and degeneracy<sup>16</sup> as well as multi-compartmental  $T_1/T_2$  effects<sup>17</sup>, cell-fibres curvature<sup>18</sup>, branching<sup>19</sup> and exchange<sup>20</sup>. However, the present suggests that these novel contrasts in soma size/density may provide a new set of biomarkers of potential great value for biomedical applications and pure neuroscience.

## ACKNOWLEDGMENTS

This work was supported by EPSRC (EP/G007748, EP/I027084/01, EP/L022680/1, EP/M020533/1, N018702), EPSRC EP/M507970/1 and European Research Council (ERC) under the European Union's Horizon 2020 research and innovation programme (Starting Grant, agreement No. 679058).

## REFERENCES

1. Novikov D S, Kiselev V G, Jespersen, S N. On modeling. *Magn. Reson. Med.*, 79(6), 3172-3193.
2. Alexander D C, Dyrby T B, Nilsson M, et al. Imaging brain microstructure with diffusion MRI: practicality and applications. *NMR Biomed.* 2017, e3841.
3. Jelescu I O, Budde M D. Design and validation of diffusion MRI models of white matter. *Front Phys* 2017, 5, 61.
4. Fieremans E, Lee H H. Physical and numerical phantoms for the validation of brain microstructural MRI: A cookbook. *Neuroimage* 2018, 182, 39-61.
5. Palombo M, Shemesh N, Ianus A, et al., Abundance of cell bodies can explain the stick model's failure to describe high b-value diffusion signal in grey matter. *Proc. Int. Soc. Magn. Reson. Med.* 2018, #1096.
6. Palombo, M., Alexander, D. C., Zhang, H. A generative model of realistic brain cells with application to numerical simulation of diffusion-weighted MR signal. *Neuroimage under review* 2018, *arXiv preprint arXiv:1806.07125*.
7. Palombo, M, Shemesh N, Ianus A, et al., A compartment based model for non-invasive cell body imaging by diffusion MRI. *Proc. Int. Soc. Magn. Reson. Med.* 2018, #0892.

8. Cook P A, Bai Y, Nedjati-Gilani S K K S, et al. Camino: open-source diffusion-MRI reconstruction and processing. In 14th scientific meeting of the international society for magnetic resonance in medicine 2004 (Vol. 2759). Seattle WA, USA.
9. Veraart J, Fieremans E, Novikov D S. On the scaling behavior of water diffusion in human brain white matter. *Neuroimage* accepted 2018, DOI:10.1016/j.neuroimage.2018.09.075
10. Yang D M, Huettner J E, Bretthorst G L, et al. Intracellular water preexchange lifetime in neurons and astrocytes. *Magn. Reson. Med.* 2018, 79(3), 1616-1627
11. Nunes D, Cruz T L, Jespersen S N, et al. Mapping axonal density and average diameter using non-monotonic time-dependent gradient-echo MRI. *J. Magn. Reson.* 2017, 277, 117-130.
12. Veraart, J., et al. Denoising of diffusion MRI using random matrix theory. *Neuroimage* 2016, 142, 394-406
13. Kellner E, Dhital B, Kiselev V G, et al. Gibbs-ringing artifact removal based on local subvoxel-shifts. *Magn. Reson. Med.* 2016, 76(5), 1574-1581.
14. <https://fsl.fmrib.ox.ac.uk/fsl>
15. BrainMaps: An Interactive Multiresolution Brain Atlas; <http://brainmaps.org>
16. Jelescu I O, Veraart J, Fieremans E, et al. Degeneracy in model parameter estimation for multi-compartmental diffusion in neuronal tissue. *NMR Biomed.* 2016, 29(1), 33-47
17. Veraart J, Novikov D S, Fieremans E. TE dependent Diffusion Imaging (TEdDI) distinguishes between compartmental T2 relaxation times. *Neuroimage* 2018, 182, 360-369.
18. Özarıslan E, Yolcu C, Herberthson M, et al. Influence of the size and curvedness of neural projections on the orientationally averaged diffusion MR signal. *Frontiers in physics* 2018, 6, 17.
19. Palombo M, Ligneul C, Najac C, et al. New paradigm to assess brain cell morphology by diffusion-weighted MR spectroscopy in vivo. *PNAS* 2016; 113(24): 6671-6676.
20. Veraart J, Fieremans E, Rudrapatna U, et al., Biophysical modeling of the gray matter: does the “stick” model hold? *Proc. Int. Soc. Magn. Reson. Med.* 2018, #1094.

## FIGURES

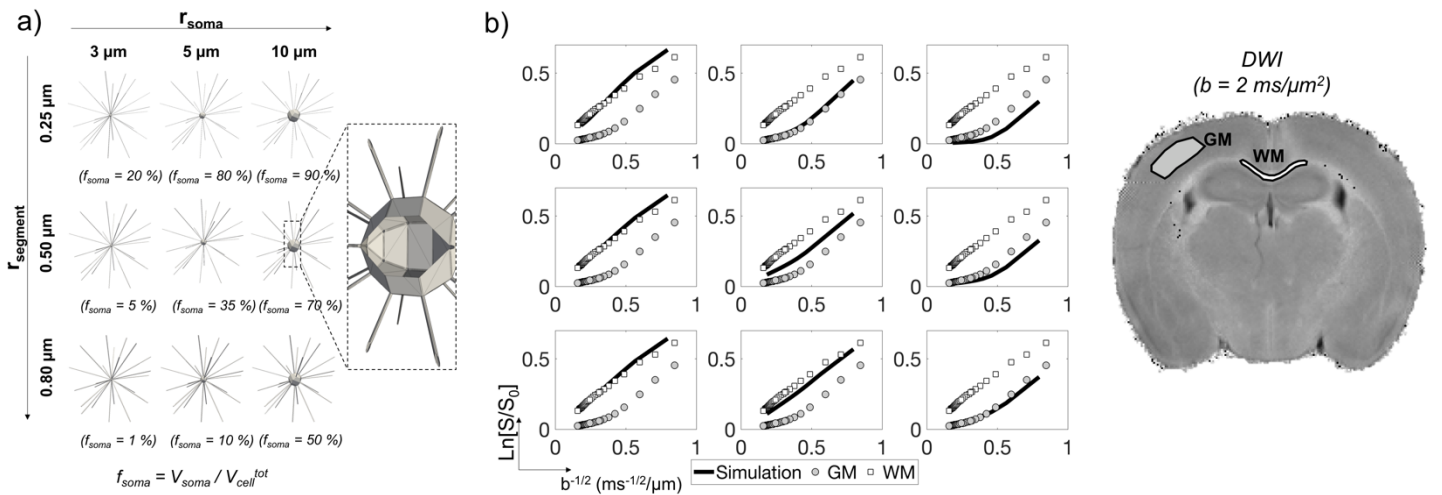


**Figure 1. Comparison of numerical simulations and experiments.** *a)* Computational model: many randomly oriented cylindrical segments of radius  $r_{\text{segment}}$  and  $200 \mu\text{m}$  long (neurites) were projected from a spherical compartment (soma) of radius  $r_{\text{soma}}$  (zoomed inset), at different volume fractions of soma  $f_{\text{soma}}$ . The intracellular diffusion of  $5 \times 10^5$  spins was simulated with bulk-diffusivity  $2 \mu\text{m}^2/\text{ms}$ . *b)* Normalised direction-averaged DW-MRI signal as a function of  $b^{-1/2}$  computed from spins' trajectories (line). Comparison with measured signal from white matter (WM) and gray matter (GM) ROIs shows very good match at  $0.2 < b^{-1/2} < 0.5$  for  $(r_{\text{soma}}, f_{\text{soma}})$  conditions:  $(3, 0.01-0.2)_{\text{WM}}$  and  $(5-10, 0.5-0.8)_{\text{GM}}$ , also suggesting negligible extra-cellular contribution for  $b^{-1/2} < 0.5$ .

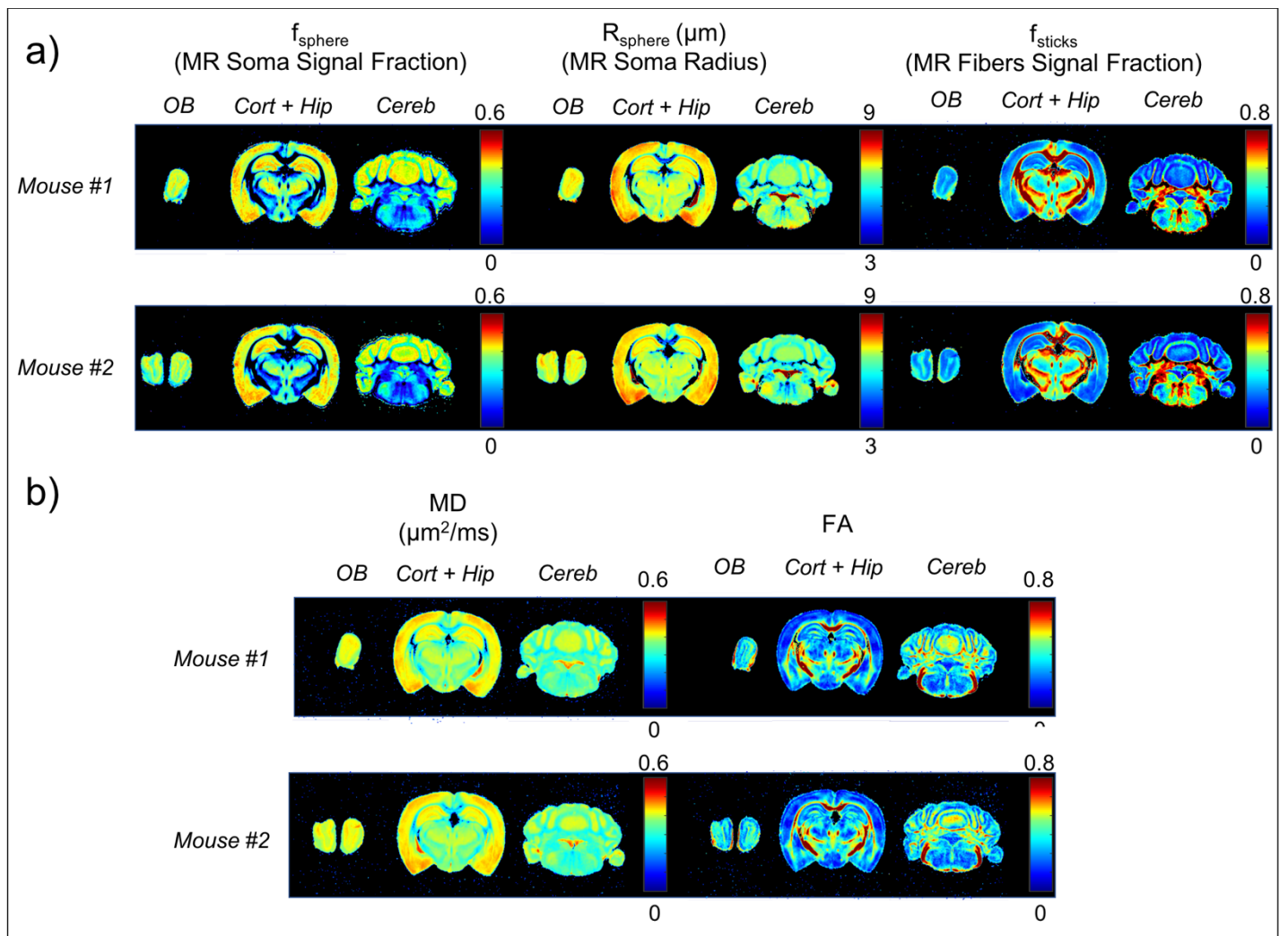


**Figure 2. Novel contrasts in soma size and density.** *a)* Voxel-wise non-linear fitting of relation [1] provided maps of MR cell body signal fraction  $f_{\text{sphere}}$  (left), radius  $R_{\text{sphere}}$  (centre), and MR cell fibers signal fraction  $f_{\text{sticks}}$  (right). Three slices of interest are displayed, containing olfactory bulb (OB), cortex (Cort), hippocampus (Hip), cerebellum (Cereb). Please note

that given a distribution of real soma size  $R$  in each voxel, the MR-measured soma radius  $R_{\text{sphere}}$  should be proportional to  $\langle R^6 \rangle / \langle R^3 \rangle$  rather than the mean radius value. *b*) DTI maps of MD and FA computed at  $b=3 \text{ ms}/\mu\text{m}^2$ .

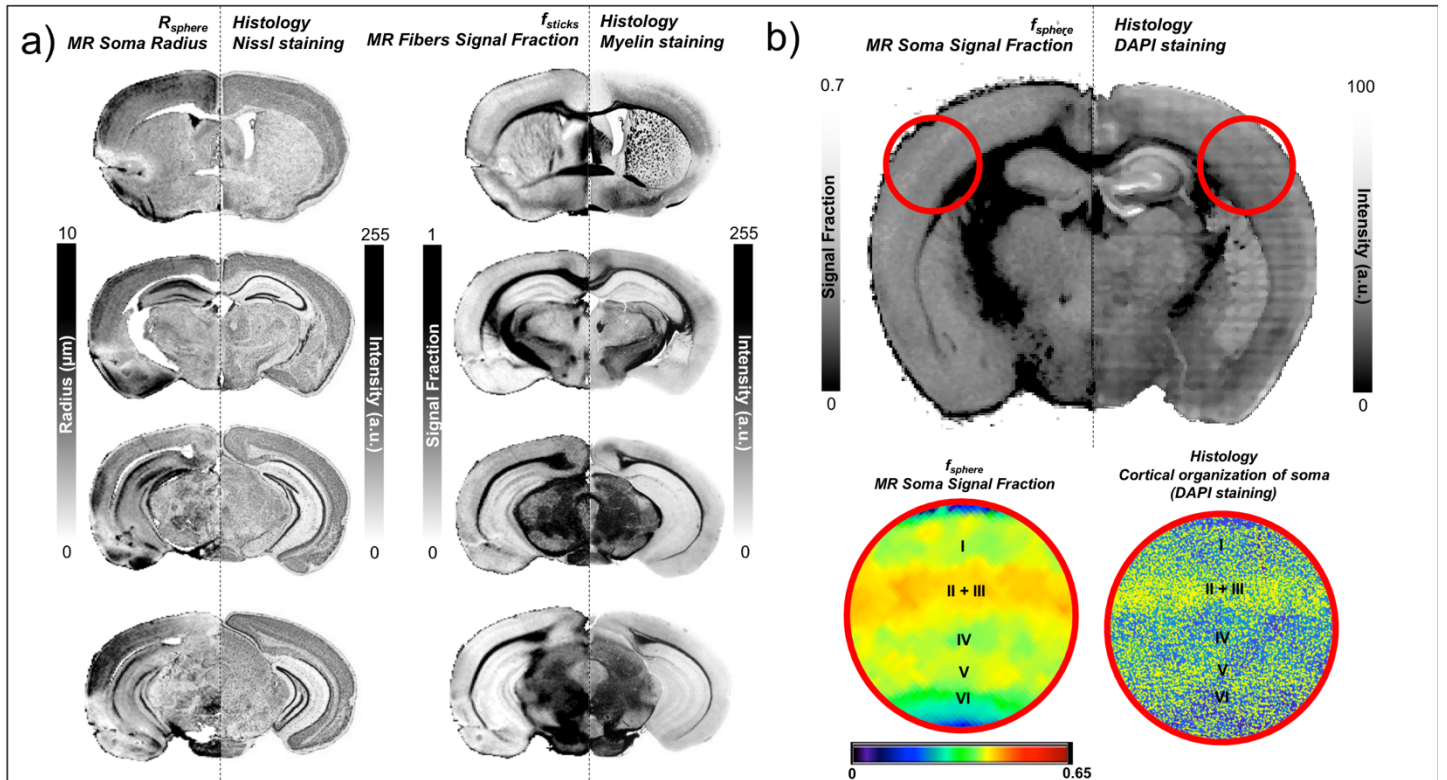


**Figure 3. Comparison with histology I.** *a*) Direct comparison of MR cell body radius  $R_{\text{sphere}}$ , and MR cell-fibers signal fraction  $f_{\text{sticks}}$ , with literature-derived histological images, adapted from<sup>15</sup>. Note the very good match of MR maps with Nissl staining (soma) images and staining of myelinated fibers. *b*) More direct comparison of MR cell body signal fraction  $f_{\text{sphere}}$  with DAPI staining (soma) of the same mouse brain. Note the very good match of the soma layering in the cortical ROI defined by the red circle, where the six cortical layers: I-VI are clearly distinguishable.

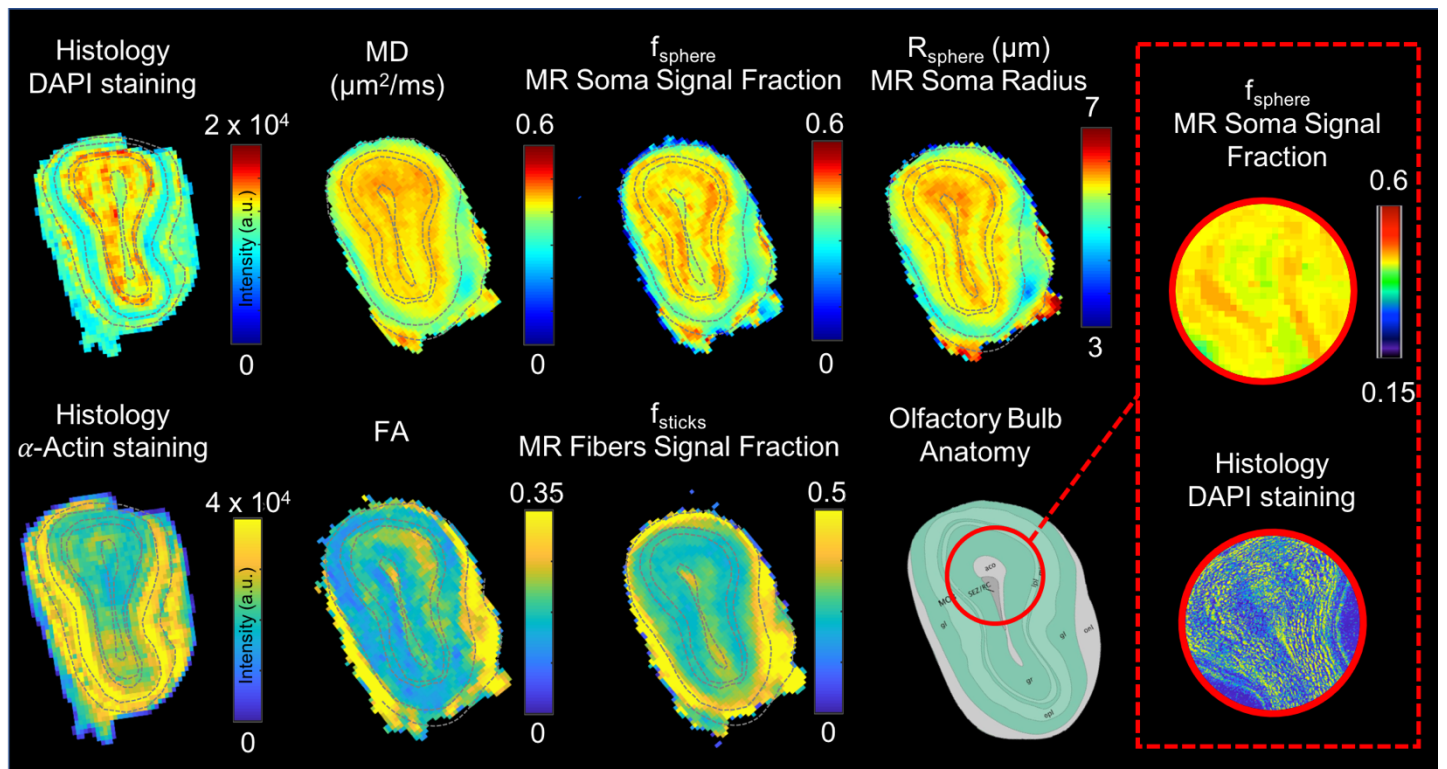


**Figure 4. Comparison with histology II.** Direct comparison of MR derived maps with histological images (DAPI staining of soma and  $\alpha$ -Actin staining of cell membrane) of the same mouse brain olfactory bulb (OB). The OB is characterized by a well-defined layering of soma (see OB anatomy from <http://atlas.brain-map.org/>) that is perfectly highlighted in maps

of MR soma signal fraction  $f_{\text{sphere}}$  and radius  $R_{\text{sphere}}$ , while it is reduced in MD map. Noticeable also the good match between cell membrane arrangement ( $\alpha$ -Actin staining) and MR cell-fibres signal fraction  $f_{\text{sticks}}$  and FA maps.

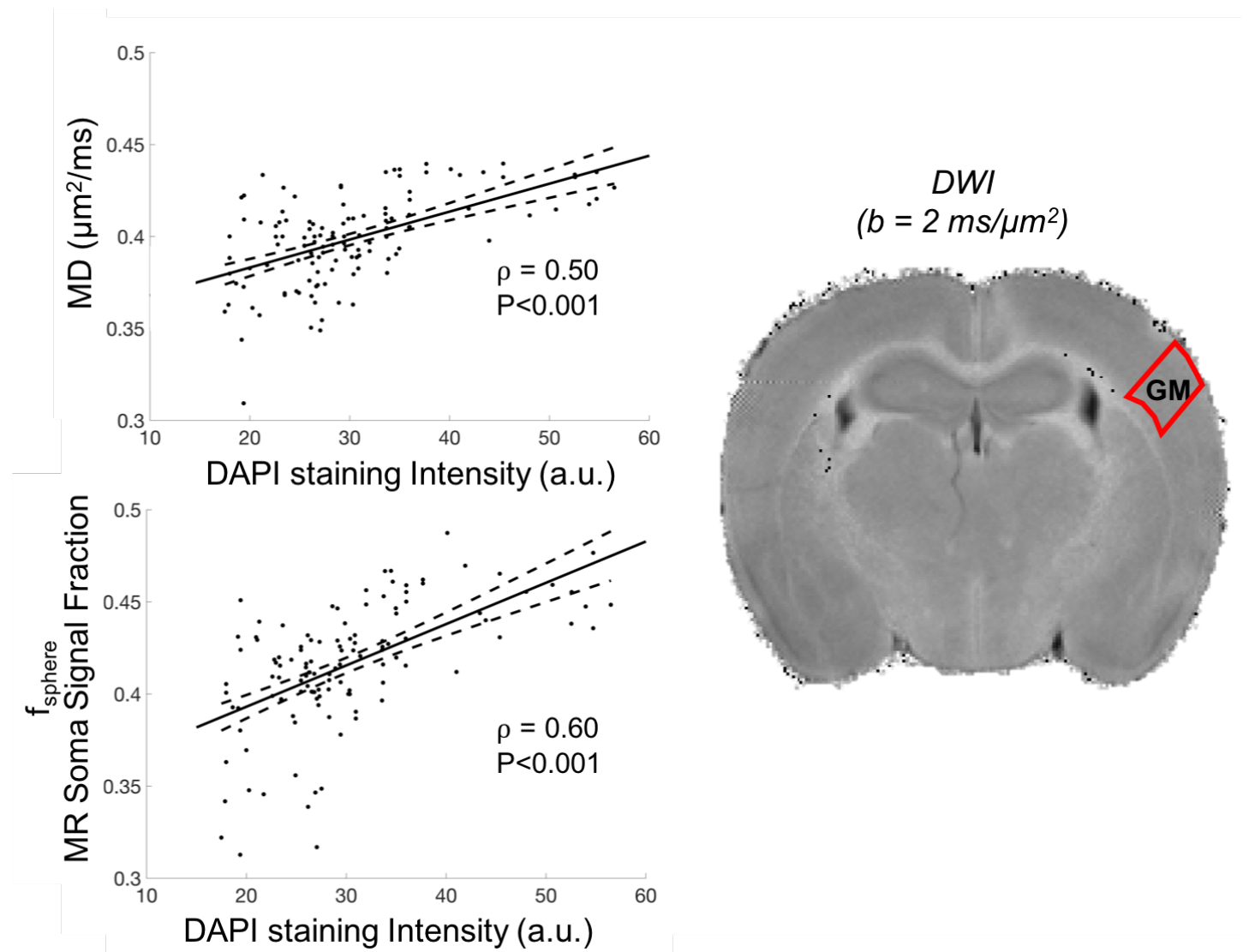


**Figure 5. Correlation of MR measured soma signal fraction with histology.** Quantitative comparison of MD values and MR soma signal fraction  $f_{\text{sphere}}$  values with DAPI staining image intensity for a ROI defined in the cortical gray matter (GM) of the same mouse brain, as shown by the reference DWI image. Linear correlation assessed by two-tailed t-test shows higher significant correlation between MR soma signal fraction  $f_{\text{sphere}}$  and DAPI staining image intensity than MD from DTI.